Nonlinear Optical Dynamics and High Reflectance of a Monolayer of Three-Level Quantum Emitters with a Doublet in the Excited State

Bairamdurdyev, D. Ya.; Malikov, R. F.; Ryzhov, I. V.; Malyshev, V. A.

Published in:
Journal of Experimental and Theoretical Physics

DOI:
10.1134/S1063776120060011

Publication date:
2020

ISSN 1063-7761, Journal of Experimental and Theoretical Physics, 2020, Vol. 131, No. 2, pp. 244–254. © Pleiades Publishing, Inc., 2020.
Russian Text © The Author(s), 2020, published in Zhurnal Eksperimental'noi i Teoreticheskoi Fiziki, 2020, Vol. 158, No. 2, pp. 269–281.

ATOMS, MOLECULES, OPTICS

Nonlinear Optical Dynamics and High Reflectance of a Monolayer of Three-Level Quantum Emitters with a Doublet in the Excited State

D. Ya. Bairamdurdyev[a], R. F. Malikov[a], I. V. Ryzhov[b,*], and V. A. Malyshev[b,c,]**

[a] *Akmulla Bashkir State Pedagogical University, Ufa, 450008 Russia*
[b] *Herzen State Pedagogical University, St. Petersburg, 198164 Russia*
[c] *Zernike Institute for Advanced Materials, University of Groningen, Groningen, 9747 AG The Netherlands*
**e-mail: igoryzhov@yandex.ru*
***e-mail: v.malyshev@rug.nl*

Received February 13, 2020; revised February 13, 2020; accepted March 3, 2020

Abstract—We study theoretically the nonlinear optical response of a monolayer of regularly arranged three-level identical quantum emitters with a doublet in the excited state to the action of a monochromatic electromagnetic field quasi-resonant to optical transitions in the emitter. The total retarded dipole–dipole interaction of the emitters is accounted for in the mean-field approximation. This interaction plays the role of a positive feedback, which (in combination with the immanent nonlinearity of emitters themselves) leads to multistability of the monolayer response. The stability of different response branches is analyzed using the Lyapunov exponents method. It is found that the instability type depends on the doublet splitting and changes from self-oscillations to chaos upon increasing the splitting. Another important property of the monolayer is its high (almost 100%) reflectance in a certain frequency range; i.e., within this range, the monolayer operates as a perfect nanometer mirror; moreover, reflection can be switched to transmission changing slightly the incident field amplitude (bistability). The possibility of application of the above mentioned monolayer optical properties in nanophotonics is discussed.

DOI: 10.1134/S1063776120060011

1. INTRODUCTION

The methods of modern micro- and nanotechnologies make it possible to obtain objects with unusual electromagnetic properties (so-called metamaterials [1–3]), among which 2D supercrystals (SCs) of semiconducting quantum dots (QDs) [4–6] and organic polymers [7] are of special interest. The SC optical properties depend on the size of QDs, their shape, chemical composition, and lattice geometry and can be purposefully controlled (see [8] and the literature cited therein). So far, the energy structure [9–11] and linear optical properties [12, 13] of 2D SCs of semiconducting QDs have been investigated. In these publications, large-scale capabilities of controlling the linear response of a 2D SC have been demonstrated, that provides a basis for application of such objects in nanophotonics.

However, nonlinear optical properties of 2D SCs have been investigated to a far lesser extent. It was shown in recent publications [14–17] that the nonlinear response of a SC of quantum emitters (QEs) with a ladder scheme [14–16] and Λ scheme of optical transitions [17] exhibits multistability, self-oscillations, and dynamic chaos. In addition, in a certain frequency range, the SC almost totally reflects the incident field, i.e., operates as an ideal nanometer-thick mirror, which, in addition, exhibits bistability. In other words, the SC reflectance can be switched from a value close to unity to almost zero and back upon minor change in the amplitude of the external or controlling field. As a result, reflectance of the monolayer forms an optical hysteresis loop when scanning back and forth of the external field amplitude.

In this study, we analyze theoretically the nonlinear optical response of a monolayer consisting of regularly spaced QEs with a doublet in the excited state (V-QEs). The role of such an emitter can be played, for example, by semiconductor QDs with a degenerate valence band in a magnetic field [18]. Because of high density of V-QEs and their large oscillator strength of transitions, the dipole–dipole interaction of V-QEs plays a crucial role in the optical response of the monolayer. Since the quantum-mechanical mean dipole moment of a V-QE depends on the current quantum state of the latter, the QE–QE interaction is also a function of this state. This ensures the positive feedback which, in combination with the immanent nonlinearity of the V-QE itself, leads to multistability of the monolayer response, self-oscillations, dynamic chaos, and a high reflectance in a certain frequency range, similar to the case of a monolayer of QEs with

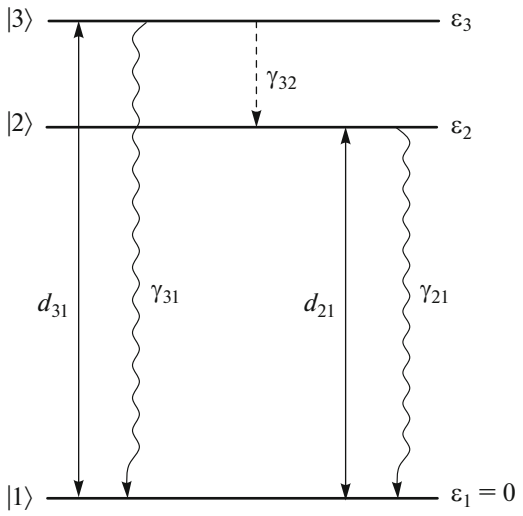

Fig. 1. Energy level diagram for an isolated V-QE, including the ground state $|1\rangle$ and a doublet $|2\rangle$ and $|3\rangle$ in the excited state: $\varepsilon_1 = \hbar\omega_1 = 0$, $\varepsilon_2 = \hbar\omega_2$, and $\varepsilon_3 = \hbar\omega_3$ are the energies of these states. Double-headed solid arrows mark the allowed optical transitions characterized by the transition dipole moments $\mathbf{d}_{21}$ and $\mathbf{d}_{31}$. Wavy arrows indicate radiative decay of the states $|2\rangle$ and $|3\rangle$ with rates γ_{21} and γ_{31} respectively. Dashed arrow denotes nonradiative relaxation of the upper state of the doublet with rate γ_{32}.

the ladder [14–16] and Λ schemes of optical transitions [17]. It should be noted in this connection that in spite of the global similarity of responses of the above-mentioned systems of three-level QEs, the physics of the optical response formation of a V-QE monolayer differs significantly from the other two analogs. In the case of a V-QE, optical transitions in it are initially coupled by the dipole–dipole interaction of the emitters, thus forming a collective system with eigenfrequencies and eigenstates deviating significantly from their initial counterparts. This fact is the main reason for differences between the optical response of a V-QE monolayer and those with other schemes of optical transitions.

The above properties of a V-QE monolayer makes this system promising for various applications in nanophotonics. Preliminary results have been reported in brief communication [19]. It should also be noted that some aspects of unstable behavior of the optical response of a thin layer with a high V-QE concentration have been considered in [20, 21].

Out approach to the description of the optical response of the monolayer of regularly spaced V-QEs is based on the system of equations for the 3×3 density matrix of an individual V-QE and the Maxwell equations for the field. The retarded dipole–dipole interactions of V-QEs is accounted for in the mean-field approximation, in which the parts of QE–QE interaction in the far and near zones are responsible for the collective shift of levels and collective radiative relaxation of states, respectively, both depending on the population difference of the V-QE levels.

The article is organized as follows. In Section 2, we present our model of the monolayer and the mathematical formalism for describing its optical response. In Section 3, we consider the steady-state solutions of master equations and analyze their stability (Section 3.1). This section also contains our results of analysis of the nature of instabilities of the monolayer optical response (Section 3.2) and a qualitative discussion of the reasons for emerging instabilities (Section 3.3). In Section 4, we consider the peculiarities of reflection of the incident field from the monolayer. In Section 5, we summarize the results and analyze the possibilities of observing the features of the V-QE monolayer optical response found for parameters of real systems.

2. MODEL AND FORMALISM

We consider a monolayer of regularly spaced identical V-QEs. The scheme of energy levels and transitions in an isolated V-QE is shown in Fig. 1, where $|1\rangle$ is the ground state with energy $\varepsilon_1 = 0$, $|2\rangle$ and $|3\rangle$ are the states of the doublet with energies $\varepsilon_2 = \hbar\omega_2$ and $\varepsilon_3 = \hbar\omega_3$, respectively. Optically allowed transitions are $|1\rangle \leftrightarrow |2\rangle$ and $|1\rangle \leftrightarrow |3\rangle$, which are characterized by the transition dipole moments $\mathbf{d}_{21}$ and $\mathbf{d}_{31}$ (we assume for simplicity that both are real-valued and have the same direction). The states $|2\rangle$ and $|3\rangle$ of the doublet decay spontaneously to the ground state $|1\rangle$ with rates γ_{21} and γ_{31}, respectively. Nonradiative relaxation in the doublet is taken into account by constant γ_{32}.

We assume that a plane wave $\mathscr{E}_0(t) = \mathbf{E}_0\cos(\omega_0 t)$ with frequency ω_0, which is quasi-resonant to optical transitions in the V-QE, is incident on the monolayer. We restrict our analysis to the normal incidence geometry and the condition of collinearity of the external field and the V-QE transition dipole moments (which is not of principal importance). In this case, all vectorial quantities can be treated as scalars.

We describe the monolayer optical response in the mean-field approximation, i.e., we assume that all dynamic variables of the V-QE and of the field are independent of the position in the monolayer. Strictly speaking, this approximation is justified only for a monolayer of infinite size. However, analysis of a finite-size system encounters serious calculation problems associated with integration of a system of nonlinear differential equations of a huge rank. As will be shown below, the solution of the nonlinear problem even in the simplest case (mean field) requires a certain carefulness in view of a possible unstable behavior of the response. Therefore, an analysis of the already nontrivial "zeroth" approximation (mean field) makes a certain sense.

The optical dynamics of V-QEs in a monolayer is governed by the master equation for the density operator $\rho(t)$ [22, 23]; in the frame of reference rotating

with frequency ω_0 of the external field, this equation has the form

$$\dot{\rho}(t) = -\frac{i}{\hbar}[H^{RWA}(t), \rho(t)] + \mathcal{L}\{\rho(t)\}, \quad (1)$$

$$H^{RWA}(t) = \hbar(\Delta_{21}\sigma_{22} + \Delta_{31}\sigma_{33}) - i\hbar[\Omega_{31}(t)\sigma_{31} + \Omega_{21}(t)\sigma_{21}] + \text{H.c.}, \quad (2)$$

$$\mathcal{L}\{\rho(t)\} = \frac{1}{2}\gamma_{31}([\sigma_{13}\rho(t), \sigma_{31}] + [\sigma_{13}, \rho(t)\sigma_{31}]) + \frac{1}{2}\gamma_{21}([\sigma_{12}\rho(t), \sigma_{21}] + [\sigma_{12}, \rho(t)\sigma_{21}]) + \frac{1}{2}\gamma_{32}([\sigma_{32}\rho(t), \sigma_{23}] + [\sigma_{32}, \rho(t)\sigma_{32}]), \quad (3)$$

$$\sigma_{ij} = |i\rangle\langle j|, \quad i, j = 1, 2, 3, \quad (4)$$

where H^{RWA} is the V-QE Hamiltonian in the rotating frame of reference, $[A, B]$ is the commutator, and $\mathcal{L}$ is the Lindblad relaxation operator [22, 23] defined by Eq. (3). In Eq. (2), $\Delta_{21} = \omega_2 - \omega_0$ and $\Delta_{31} = \omega_3 - \omega_0$ are the detunings of the external field frequency from the frequencies of the $2 \leftrightarrow 1$ and $3 \leftrightarrow 1$ transitions. Further, $\Omega_{31}(t) = d_{31}E(t)/\hbar = \Omega(t)$ and $\Omega_{21}(t) = d_{21}E(t)/\hbar = \mu\Omega(t)$ ($\mu = d_{21}/d_{31}$) are the Rabi amplitudes of the field acting on the V-QE, which correspond to the $3 \leftrightarrow 1$ and $2 \leftrightarrow 1$ transitions. The Rabi amplitude $\Omega(t)$ is the sum of the Rabi amplitudes $\Omega_0 = d_{31}E_0/\hbar$ of the external field and of the field produced by other V-QEs in place of the given V-QE. In the mean-field approximation, $\Omega(t)$ is given by the following equation [16] (here and in what follows, we suppress the time dependence of all variables):

$$\Omega = \Omega_0 + (\gamma_R - i\Delta_L)(\rho_{31} + \mu\rho_{21}). \quad (5)$$

The expressions for constants γ_R and Δ_L depend on the relationship between the lateral lattice size Na (N is the lateral number of sites and a is the lattice constant) and radiation wavelength $\lambda = 2\pi c/\omega_0$, c being the speed of light. For a simple square lattice with lateral size $Na \ll \lambda$ (pointlike system), the quantities γ_R and Δ_L are given by [16]

$$\gamma_R = \frac{3}{8}\gamma_{31}N^2, \quad (6)$$

$$\Delta_L = 3.39\gamma_{31}\left(\frac{\lambda\!\!\!^{-}}{a}\right)^3, \quad (7)$$

where $\lambda\!\!\!^{-} = \lambda/2\pi$. In the opposite case of $Na \gg \lambda$ (extended system), we have [16]

$$\gamma_R = 4.51\gamma_{31}\left(\frac{\lambda\!\!\!^{-}}{a}\right)^2, \quad (8)$$

$$\Delta_L = 3.35\gamma_{31}\left(\frac{\lambda\!\!\!^{-}}{a}\right)^3. \quad (9)$$

As follows from Eqs. (6) and (8), the constant γ_R for a pointlike system depends on the total number N^2 of V-QEs in the lattice, while the value of γ_R for an extended system is proportional to the number of V-QEs within an area of size $\lambda\!\!\!^{-2}$. Here, it is worth to note that γ_R is nothing else that the Dicke superradiance constant [16, 24–26] responsible for collective relaxation of V-QEs in the monolayer. The parameter Δ_L is almost independent of the lattice size and is nothing else that the static dipole–dipole interaction of V-QEs. It should be emphasized that for $\lambda\!\!\!^{-} \gg a$ (in the case of interest for our analysis), the relation $\Delta_L \gg \gamma_R$, which is crucial for the optical dynamics of the monolayer (see below), holds irrespective of the lattice size.

Within the basis of states $|1\rangle$, $|2\rangle$, and $|3\rangle$, Eq. (1) represents the following system of equations for the matrix elements $\rho_{\alpha\beta}$ ($\alpha, \beta = 1, 2, 3$):

$$\dot{\rho}_{11} = \gamma_{21}\rho_{22} + \gamma_{31}\rho_{33} + \Omega^*\rho_{31} + \Omega\rho_{31}^* + \mu(\Omega^*\rho_{21} + \Omega\rho_{21}^*), \quad (10)$$

$$\dot{\rho}_{22} = \gamma_{32}\rho_{33} - \gamma_{21}\rho_{22} - \mu(\Omega^*\rho_{22} + \Omega\rho_{21}^*), \quad (11)$$

$$\dot{\rho}_{33} = -(\gamma_{31} + \gamma_{32})\rho_{33} - \Omega^*\rho_{31} - \Omega\rho_{31}^*, \quad (12)$$

$$\dot{\rho}_{31} = -\left[i\Delta_{31} + \frac{1}{2}(\gamma_{31} + \gamma_{32})\right]\rho_{31} + \Omega(\rho_{33} - \rho_{11}) + \mu\Omega\rho_{32}, \quad (13)$$

$$\dot{\rho}_{21} = -\left[i\Delta_{21} + \frac{1}{2}\gamma_{21}\right]\rho_{21} + \mu\Omega(\rho_{22} - \rho_{11}) + \Omega\rho_{32}^*, \quad (14)$$

$$\dot{\rho}_{32} = -\left[i\Delta_{32} + \frac{1}{2}(\gamma_{31} + \gamma_{21} + \gamma_{32})\right]\rho_{32} - \mu\Omega^*\rho_{31} - \Omega\rho_{21}^*. \quad (15)$$

It should be noted that Eqs. (10)–(15) conserve the total population ($\rho_{11} + \rho_{22} + \rho_{33} = 1$); i.e., we disregard all other population relaxation channels except the radiative channel. Dephasing of states, differing from radiative one, is also neglected.

3. RESULTS

We performed numerical calculations of the monolayer optical response, choosing the constants, which determine γ_R and Δ_L, similar to those of 2D SCs of semiconductor QDs [16]: $\lambda\!\!\!^{-} \sim 100$–$200$ nm, $a \sim 10$–20 nm, and $\gamma_{31} \approx 3 \times 10^9\ \text{s}^{-1}$. Then the typical values of parameters $\gamma_R = 100\gamma_{31}$ and $\Delta_L = 1000\gamma_{31}$. The relaxation constant γ_{32} in the doublet was set to be fixed ($\gamma_{32} = 0.01\gamma_{31}$). In fact, since $\gamma_{32} \ll \gamma_{31}$, this constant almost does not affect the results. The variable quantities were the doublet splitting Δ_{32} and the detuning from resonance Δ_{31}. All calculations were carried out assuming that $\gamma_{21} = \gamma_{31}$ ($\mu = 1$). In what follows, all fre-

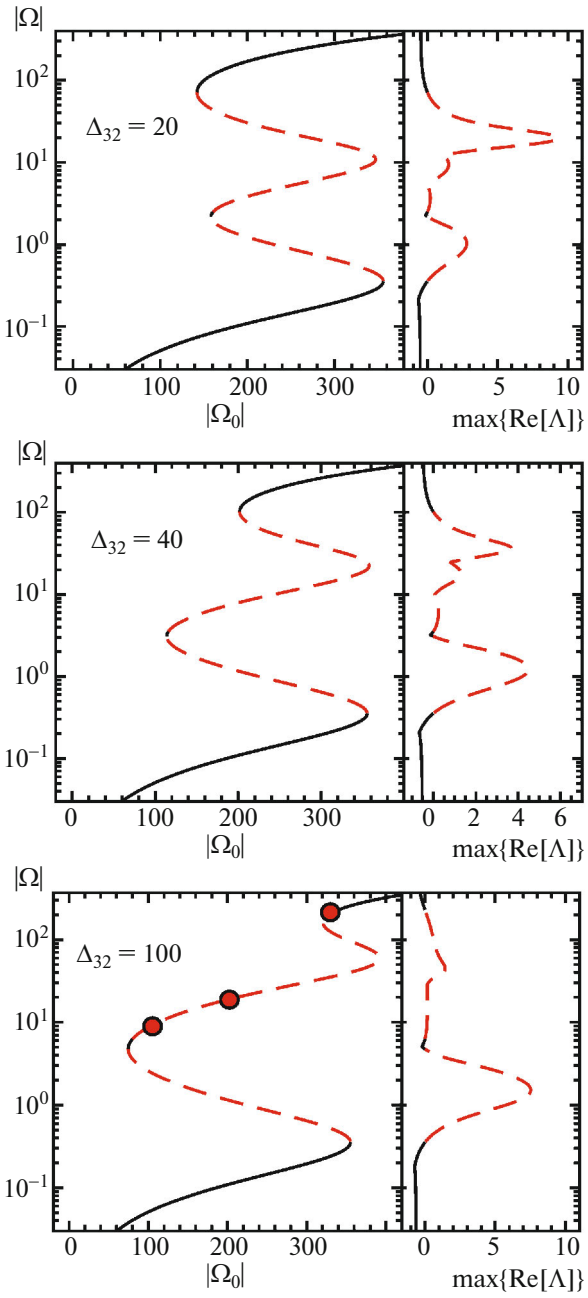

Fig. 2. Steady-state optical response of the monolayer under excitation of the latter into the resonance with the transition $1 \leftrightarrow 3$ ($\Delta_{31} = 0$) in an isolated V-QE. Left parts of the panels show the steady-state solution $|\Omega|(|\Omega_0|)$ to the system of equations (5) and (10)–(15), which was obtained using the parametric method (see Appendix A) for values of the doublet splitting Δ_{32} = (a) 20, (b) 40, and (c) 100. Solid (dashed) fragments of the curves correspond to stable (unstable) parts of steady-state solutions. Right parts of the panels show the maximal Lyapunov exponent max{Re[Λ]}. Circles in the lower panel indicate the points of the steady-state solution, for which the optical dynamics of the monolayer response is calculated in Section 3.2. The remaining parameters of the monolayer are given in the text. All quantities are given in units of γ_{31}.

quency dimension quantities are given in units of γ_{31}, while time is in units of γ_{31}^{-1}.

3.1. Steady-State Solutions

As the first step of our analysis of the V-QE monolayer optical response, we consider steady-state solutions to the master equations (10)–(15), formally setting in them to zero the time derivatives. Here, it is appropriate to clarify that stationarity of the solution does not imply its stability. As will be shown below, a steady-state solution can be either stable or unstable.

In order to find steady-state solutions, we used the parametric method [16] described in Appendix A. The results of calculations are shown in Figs. 2 and 3. The result presented in Fig. 2 was obtained for excitation of the monolayer into the resonance with the $1 \leftrightarrow 3$ transition ($\Delta_{31} = 0$) in an isolated V-QE, while the one in Fig. 3 corresponds to the excitation into the center of the doublet ($\Delta_{31} = \Delta_{32}/2$). It should be noted that for a V-QE in the mean field ("dressed" V-QE), the true resonance conditions are $\Delta_{31} = \Delta_{32}/2$ and $\Delta_{31} = 2\Delta_L$ (see Appendix B). Therefore, only the excitation to the center of the doublet, being nonresonant for an isolated V-QE, turns out to be resonant for the dressed V-QE.

The doublet splitting Δ_{32} was chosen as the variable parameter. Each panel in Figs. 2 and 3 consists of two parts. The 1eft one shows the dependence of the Rabi magnitude $|\Omega|$ of the field in the monolayer on the Rabi magnitude $|\Omega_0|$ of the external field. The right-hand part shows the dependence of the maximal Lyapunov exponent of the solution on $|\Omega|$ (see below).

As follows from Fig. 2, the dependence of $|\Omega|$ on $|\Omega_0|$, in a certain interval of changing $|\Omega_0|$, is multivalued for all values of the doublet splitting Δ_{32}, which means multistability of the monolayer response. Herewith, the character of the steady-state solution (stable/unstable) differs in its different parts: the fragments depicted by solid curves are stable, while shown by dashed curves are unstable. Stability of a given solution was analyzed using Lyapunov exponents [27, 28]; namely, we considered eigenvalues Λ_k ($k = 1, 2, ..., 8$) of the Jacobi matrix of the right-hand sides of Eqs. (10)–(15) as a function of $|\Omega|$. The Lyapunov exponent Λ_k with the maximal real part max{Re[Λ]} determines whether the solution is stable: if max{Re[Λ]} < 0, the solution is stable, and vice versa. In other words, in the former case, small deviations from the steady-state solution will decay, returning the system back to the steady state, and will grow up in the latter case, taking the system away from this state. The maximal Lyapunov exponent max{Re[Λ]} is shown on the right-hand sides of the panels in Figs. 2 and 3. Interestingly, not only the branches with a negative slope are unstable (which is usually the case), but also those with a positive slope.

It should be noted that the behavior of the steady-state response of the monolayer under excitation into

the doublet center ($\Delta_{31} = \Delta_{32}/2$), shown in Fig. 3, differs substantially from the one under excitation into the resonance with the $1 \leftrightarrow 3$ transition ($\Delta_{31} = 0$) in an isolated V-QE. Namely, in the former case, as opposed to the latter, the steady-state solutions do not exhibit multivaluedness in the steady state for any doublet splitting. In particular, for $\Delta_{32} = 20$, 100, the dependence of $|\Omega|$ on $|\Omega_0|$ is single-valued. Moreover, steady-state solutions are essentially unstable. The character of instabilities of steady-state solutions will be considered in the next section.

3.2. Dynamics

In this section, we analyze the character of instabilities in the monolayer optical response for the two types of its excitation, which were considered above: in resonance with the $1 \leftrightarrow 3$ transition in an isolated V-QE ($\Delta_{31} = 0$) and in the center of the doublet splitting ($\Delta_{31} = \Delta_{32}/2$). For this purpose, we integrate numerically the system of dynamic equations (5) and (10)–(15). Here, it should be emphasized that this system of equations involves several significantly different time scales ($\gamma_{31}^{-1} \gg \gamma_R^{-1} \gg \Delta_L^{-1}, |\Omega_0|^{-1}$); i.e., it belongs to the class of so-called stiff differential equations, for which the traditional Runge–Kutta method turns out to be inconsistent. For their integration, we used special codes like ODE23tb of the MATLAB package.

The initial conditions were chosen depending on the type of monolayer excitation. In the case of excitation into the resonance with the $1 \leftrightarrow 3$ transition in an isolated V-QE ($\Delta_{31} = 0$), we chose as initial points those belonging to the steady-state solution (see Fig. 2, lower panel). It should be noted that these points are inaccessible from the ground state of the V-QE, but they can be reached by exciting the stable part of the upper branch of the steady-state solution and then by sweeping down adiabatically the external field Rabi magnitude $|\Omega_0|$. In the case of excitation into the doublet splitting center ($\Delta_{31} = \Delta_{32}/2$), the unstable solutions of the upper branch of the steady-state characteristic can be reached from the ground state of the V-QE, $\rho_{11}(0) = 1$.

The results of calculations are shown in Figs. 4 and 5 (excitation conditions are detailed in the figure captions). The left panels illustrate the dynamics of the Rabi magnitude $|\Omega|$ of the field in the monolayer, which demonstrates the same scenario irrespective of doublet splitting Δ_{32} and excitation conditions: after a certain transient stage, the signal acquires a stable form (attractor) [29–31]. Middle panels in Figs. 4 and 5 show the Fourier spectrum of the attractor, $|\int \exp(i\omega t)\Omega(t)dt|$, while right panels display the attractor phase trajectory on the (Re[Ω], Im[Ω]) plane.

The nature of the attractor dramatically depends on the type of excitation and initial conditions. For example, in the case of monolayer excitation into the resonance with the $1 \leftrightarrow 3$ transition in an isolated V-QE ($\Delta_{31} = 0$) and selected initial conditions (on the upper unstable branch of the steady-state solution; see Fig. 2, lower panel), we observe the following. For the point ($|\Omega_0| = 100$, $|\Omega| = 8.7879$), the Fourier spectrum of the attractor contains a finite number of harmonics, and its phase trajectory is a closed curve, indicating that

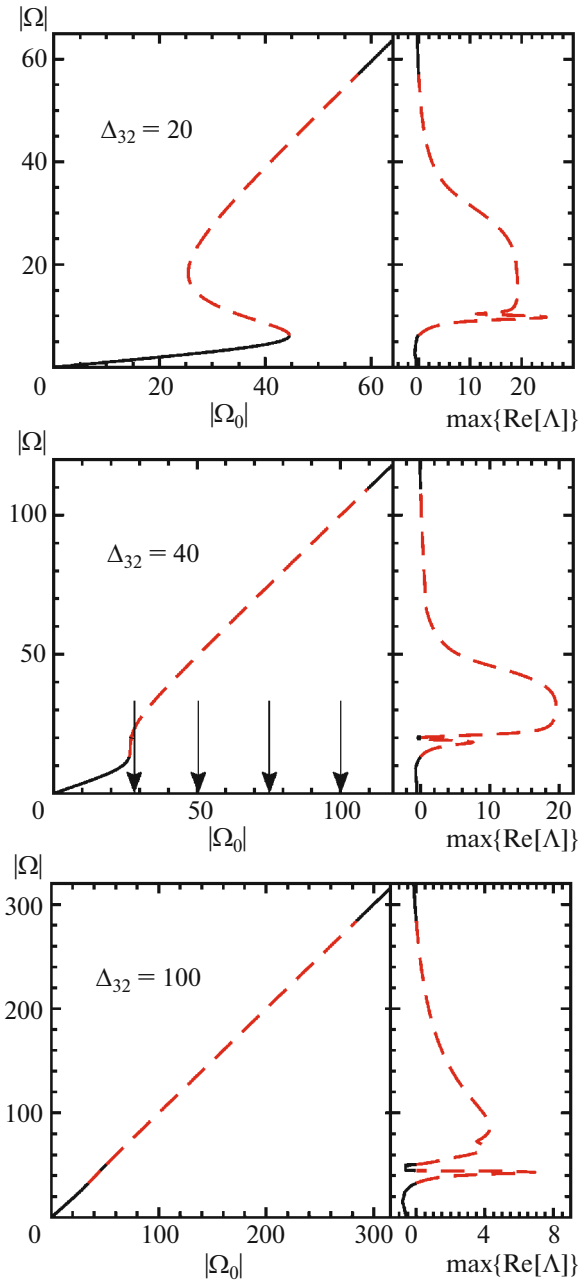

Fig. 3. Same as in Fig. 2, but only for the case of excitation of the monolayer into the center of doublet splitting ($\Delta_{31} = \Delta_{32}/2$) in an isolated V-QE. Arrows in the middle panel show the values of the Rubi magnitude $|\Omega_0|$ of the external field, for which the optical dynamics of the monolayer response is calculated in Section 3.2.

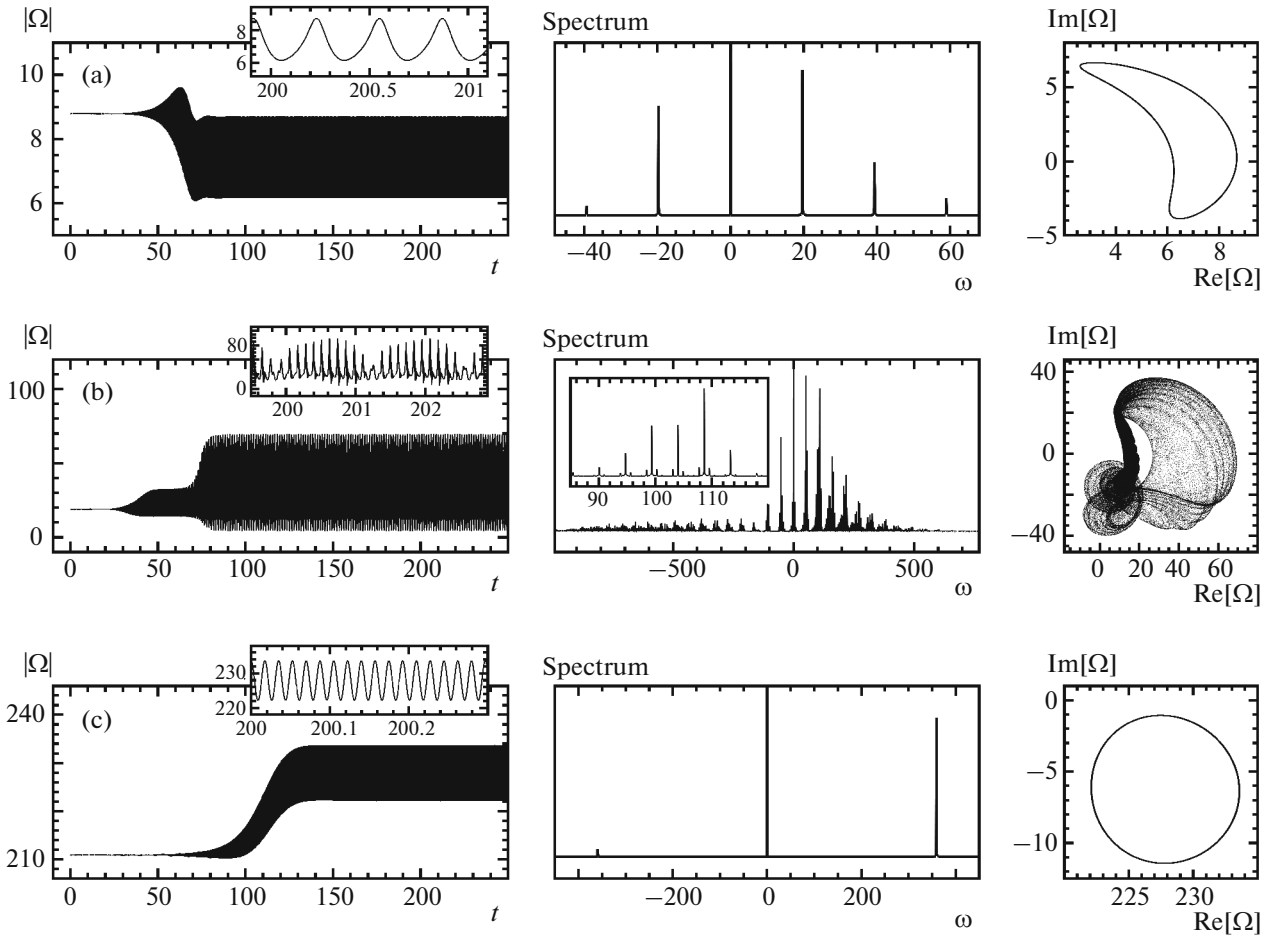

Fig. 4. Optical dynamics of the monolayer under its excitation into resonance with the transition $1 \leftrightarrow 3$ ($\Delta_{31} = 0$). Left panels illustrate the dynamics of the field $|\Omega|(t)$ in the monolayer obtained by solving the system of equations (5) and (10)–(15) for the points on the steady-state curve shown in Fig. 2 (lower panel): (a) $|\Omega_0| = 100$, $|\Omega| = 8.7879$; (b) $|\Omega_0| = 200$, $|\Omega| = 18.9398$; and (c) $|\Omega_0| = 330$, $|\Omega| = 210.9087$. Middle panels show the Fourier spectrum of the attractor. Right panels show the phase portrait of the attractor on the (Re[Ω], Im[Ω]) plane. The insets show details of the main curves. The quantities with dimensions of frequency are given in units of γ_{31}, time is measured in units of γ_{31}^{-1}.

the attractor in this case is a limit cycle [29–31]. For ($|\Omega_0| = 2100$, $|\Omega| = 18.9398$) as the initial point, the Fourier spectrum consists of a set of incommensurate frequencies. Accordingly, the phase trajectory in this case represents an open curve lying on a torus in the 8D phase space of the system considered. Finally, for point ($|\Omega_0| = 330$, $|\Omega| = 210.9087$), the attractor is again in a limit cycle.

The monolayer optical dynamics under excitation into the doublet splitting center ($\Delta_{31} = \Delta_{32}/2$), presented in Fig. 3, was calculated for conditions when the V-QE at the initial instant was in the ground state, $\rho_{11}(0) = 1$. Calculations were performed for four values of the Rabi magnitude $|\Omega_0|$ of the external field, shown by arrows in Fig. 3 (middle panel). In this case, the following types of attractors are realized. For $|\Omega_0| = 26$ and $|\Omega_0| = 100$, the system evolves over time to the limit cycle. For the other two values, $|\Omega_0| = 50$ and $|\Omega_0| = 75$, the attractors are of chaotic nature: their spectra are formed by a continuous set of frequencies, and phase trajectories densely fill a finite area on the phase plane (Re[Ω], Im[Ω]).

Based on the above, we can conclude that the nature of the optical dynamics of the monolayer dramatically depends on the initial and excitation conditions. For certain values of the Rabi magnitude $|\Omega_0|$ of the external field, one dynamic regime (attractor) changes to another. The system is said to experience bifurcation [29–31]. In the case of excitation of the monolayer into resonance with the $1 \leftrightarrow 3$ transition in an isolated V-QE ($\Delta_{31} = 0$), we observe the Andronov–Hopf bifurcations [29–31] limit cycle–limit cycle. Under excitation to the doublet splitting center, limit cycle–chaos–limit cycle bifurcations occur. The points at which bifurcations take place are determined from the calculation of the bifurcation diagram of the response, which is a stand-alone problem.

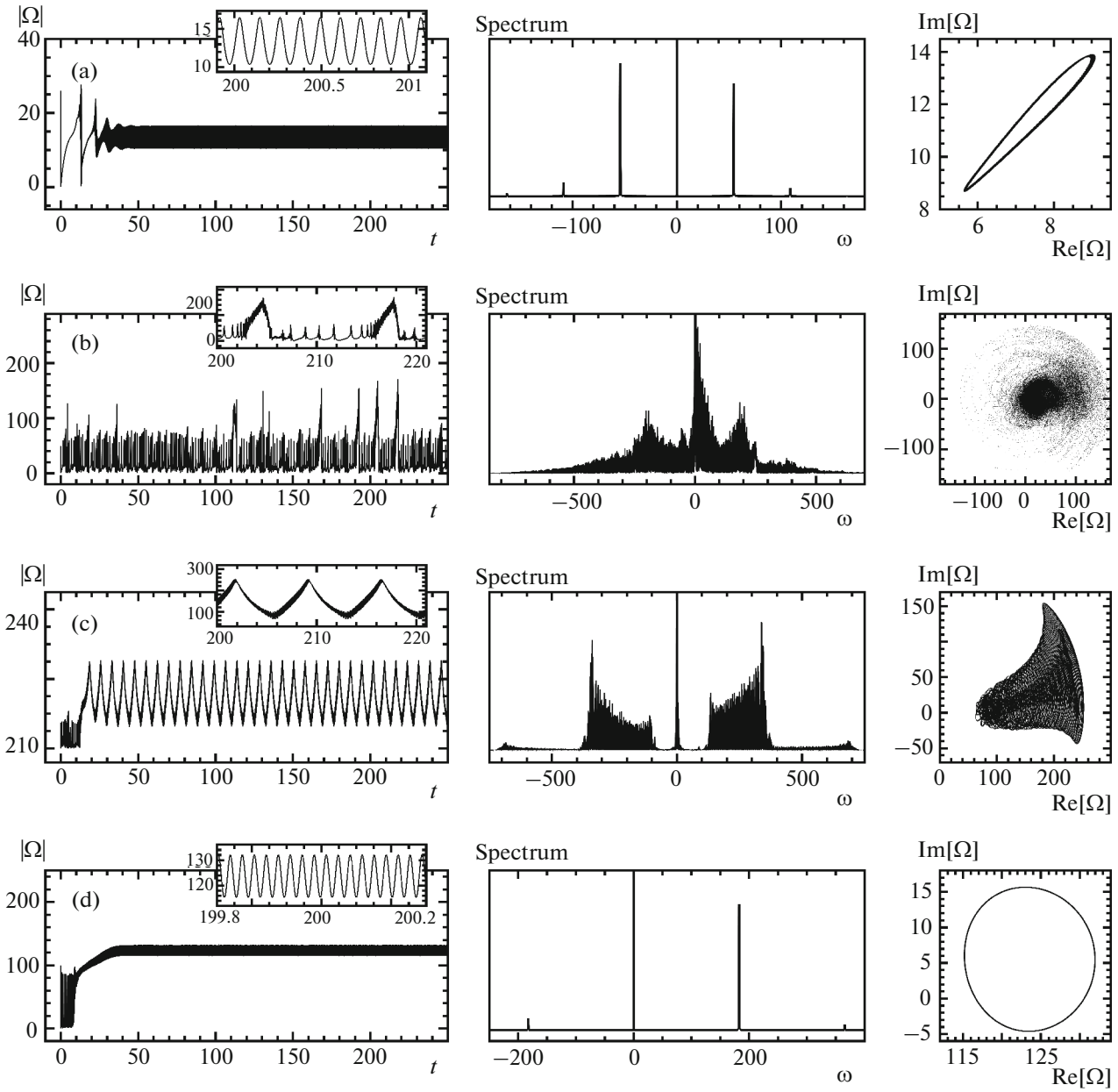

Fig. 5. Same as in Fig. 4, but only for the case of excitation of the monolayer into the doublet splitting center ($\Delta_{31} = \Delta_{32}/2$) for the Rabi magnitude $|\Omega_0|$ of the external field indicated by arrows in Fig. 3 (middle panel): (a) $|\Omega_0| = 26$; (b) $|\Omega_0| = 50$; (c) $|\Omega_0| = 75$; and (d) $|\Omega_0| = 100$ for the initial condition $\rho_{11}(0) = 1$.

3.3. Qualitative Reasoning

The results considered above show that the monolayer optical response can be multistable as well as unstable, demonstrating self-oscillations and dynamic chaos. The reason for such a behavior is the (acting) field produced by the other emitters in place of a given one. This field depends on the current quantum state of emitters, which provides a positive feedback ultimately leading to multivaluedness and instability of the monolayer response. Note that a thin layer of two-level emitters does not exhibit such properties (except bistability) [32–42].

In this section, we consider qualitatively principal nonlinearities responsible for extraordinary properties of the optical response of the V-QE monolayer. This is manifested in the most explicit form in the equations for optical coherences ρ_{31} and ρ_{21}. Substituting Eq. (5) for Ω into Eqs. (13) and (14), we obtain

$$\dot{\rho}_{31} = -\left[i(\Delta_{31} + \Delta_L Z_{31}) + \frac{1}{2}(\gamma_{31} + \gamma_{32}) - \gamma_R Z_{31} \right]\rho_{31} + \mu(\gamma_R - i\Delta_L)Z_{31}\rho_{21} + \mu(\gamma_R - i\Delta_L)(\rho_{31} + \mu\rho_{21})\rho_{32} + \Omega_0(Z_{31} + \mu\rho_{32}), \quad (16)$$

$$\dot{\rho}_{21} = -\left[i(\Delta_{21} + \mu^2 \Delta_L Z_{21}) + \frac{1}{2}\gamma_{21} - \mu^2 \gamma_R Z_{21} \right] \rho_{21}$$
$$+ \mu(\gamma_R - i\Delta_L) Z_{21} \rho_{31} + (\gamma_R - i\Delta_L)(\rho_{31} + \mu\rho_{21})\rho_{32}^* \quad (17)$$
$$+ \Omega_0(\mu Z_{21} + \rho_{32}^*).$$

Let us consider the first terms in the right-hand sides of Eqs. (16) and (17). Note that the terms $\Delta_L Z_{31}$, $\mu^2 \Delta_L Z_{21}$, $\gamma_R Z_{31}$, and $\mu^2 \gamma_R Z_{21}$ in the square brackets, which do not appear in equations for an isolated V-QE, are a direct consequence of the field acting on V-QEs in the monolayer. As is seen, this field leads, first, to a shift of the resonance frequencies of the V-QE by $\Delta_L Z_{31}$ and $\mu^2 \Delta_L Z_{21}$ for the transitions $1 \leftrightarrow 3$ and $1 \leftrightarrow 2$, respectively:

$$\omega_3 \to \omega_3 + \Delta_L Z_{31}, \quad \omega_2 \to \omega_2 + \mu^2 \Delta_L Z_{21},$$

and, second, to an additional (collective) broadening of these transitions:

$$(1/2)(\gamma_{31} + \gamma_{32}) \to (1/2)(\gamma_{31} + \gamma_{32} - \gamma_R Z_{31}),$$
$$(1/2)\gamma_{21} \to (1/2)(\gamma_{21} - \mu^2 \gamma_R Z_{21}).$$

It should be emphasized that these shifts and broadenings depend on the population difference of the transitions, i.e., are of dynamic nature.

The second terms in the right-hand sides of Eqs. (16) and (17) describe the coupling of optical transitions $1 \leftrightarrow 3$ and $1 \leftrightarrow 2$ through the secondary field and, hence, are proportional to its amplitude $\gamma_R - i\Delta_L$, as well as to the populations difference Z_{31} and Z_{21}. Because of the transition frequency shifts and transition interrelation, the eigenfrequencies of the dressed V-QE (in the monolayer) differ significantly from the bare values ω_3 and ω_2 in an isolated V-QE (see Appendix B for details).

After the external field is switched on, the energy levels of the dressed V-QE start to populate and, hence, to shift, changing simultaneously the resonance conditions and leading to a redistribution of populations. The mutual influence of these factors is the main reason for the complex monolayer optical dynamics.

4. REFLECTION

In our analysis of the nonlinear response of the V-QE monolayer, we used field Ω acting on V-QEs. In experiment, as a rule, the reflected (Ω_{refl}) or transmitted field (Ω_{tr}) is measured, which differs from the acting field Ω. The fields Ω_{refl} and Ω_{tr} are determined by a part of Ω in the far zone and are given by (see, for example, the literature cited in [16, 26, 36])

$$\Omega_{\text{refl}} = \gamma_R(\rho_{31} + \mu\rho_{21}), \quad (18)$$

$$\Omega_{\text{tr}} = \Omega_0 + \gamma_R(\rho_{31} + \mu\rho_{21}). \quad (19)$$

We are interested, in particular, in reflectance of the monolayer or, in other words, in the reflection coefficient R of the light flux (power), which is defined as

$$R = \left| \frac{\Omega_{\text{refl}}}{\Omega_0} \right|^2. \quad (20)$$

4.1. Linear Regime

Let us first consider the linear regime of reflection ($\Omega_0 \ll 1$, $\rho_{11} \approx 1$). To this end, we keep in Eqs. (13) and (14) only the terms linear in Ω_0. We also restrict our analysis to the steady-state regime. Substituting the linear solution to equations for ρ_{31} and ρ_{21} into Eq. (20), we obtain the following expression for the reflection coefficient R:

$$R = \gamma_R^2 \left| \frac{\mu^2 \left[i\Delta_{31} + \frac{1}{2}(\gamma_{31} + \gamma_{32}) \right] + i\Delta_{21} + \frac{1}{2}\gamma_{21}}{\left[i(\Delta_{31} - \Delta_L) + \frac{1}{2}(\gamma_{31} + \gamma_{32}) + \gamma_R \right] \left[i(\Delta_{21} - \mu^2 \Delta_L) + \frac{1}{2}\gamma_{21} + \mu^2 \gamma_R \right] - \mu^2 (\gamma_R - i\Delta_L)^2} \right|^2. \quad (21)$$

The dependence $R(\Delta_{31})$ in a wide range of variation of the doublet splitting Δ_{32} is shown in Fig. 6. As is seen, the monolayer reflectance has two peaks at eigenfrequencies of the dressed V-QE. The weak reflection peak ($R \ll 1$) for $\Delta_{31} \approx \Delta_{32}/2$ originates from the antisymmetric ("dark") state of the dressed V-QE, while the strong peak ($R \approx 1$) at $\Delta_{31} \approx 2\Delta_L = 2000$ originates from the symmetric ("bright") state (see Appendix B).

4.2. Nonlinear Regime

Let us now consider the nonlinear reflection regime. Figure 7 shows the dependence of the monolayer reflection coefficient R on the intensity $|\Omega_0|^2$ of the external field, calculated for different values of the detuning from resonance Δ_{31} in the vicinity of the total reflection peak ($R \approx 1$). The results are almost independent of the doublet splitting Δ_{32}. Therefore, for illustration, we consider only the data obtained for $\Delta_{32} = 100$ (cf. Fig. 6). It follows from Fig. 7 that in the detuning range above the linear reflection peak at $\Delta_{31} = 2\Delta_L = 2000$, the reflection coefficient R is a three-valued function of the intensity $|\Omega_0|^2$. The analysis of stability (of Lyapunov exponents) of different branches shows that the branches with a negative slope are unstable (thus implying bistability of reflection),

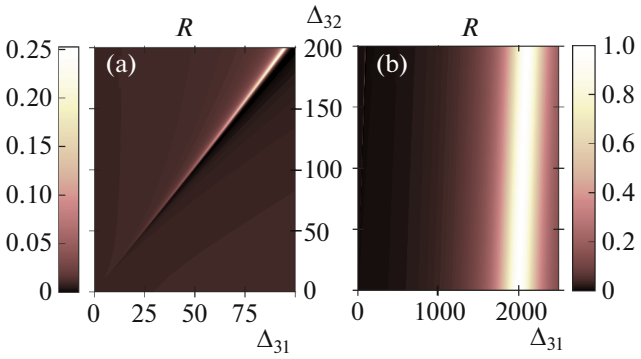

Fig. 6. Contour plot of the linear reflection coefficient R of the monolayer, calculated using Eq. (9). A low-intensity reflection peak appears in the range of $\Delta_{31} \approx \Delta_{32}/2$ (a); a peak of the almost total reflection ($R \approx 1$) occurs in the range of $\Delta_{31} \approx 2\Delta_L$ (b).

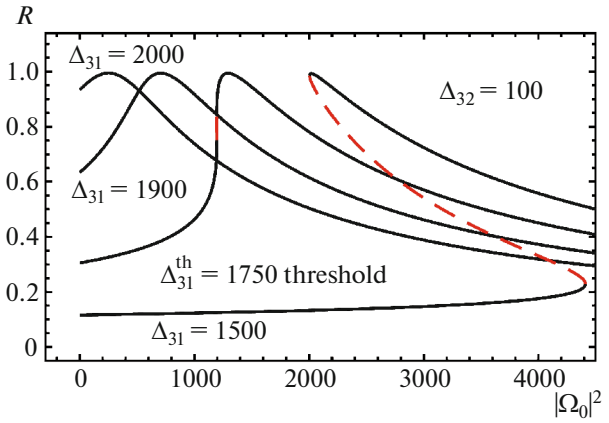

Fig. 7. Bistability of the (nonlinear) reflection coefficient R of the monolayer as a function of detuning Δ_{31} from resonance, the values of which are shown at the curves. The curves were obtained from the solution of the steady-state problem by the method described in Appendix A. Doublet splitting $\Delta_{32} = 100$; $\Delta_{31}^{th} = 1750$ is the bistability threshold. Solid (dashed) fragments of the curve correspond to stable (unstable) regions of R.

i.e., the monolayer reflectance can be switched from a low to a high value and back by a small variation of the external field intensity. In other words, in the region of the strong reflection peak ($R \approx 1$), the monolayer can operate as a bistable mirror. The bistability threshold (emergence of a three-valued solution) turns out to be $\Delta_{31}^{th} = 1750$ for the adopted values of parameters. This value coincides with a high degree of accuracy with that for a two-level QE model where $\Delta_{21}^{th} = \sqrt{3}\Delta_L = 1732$ [26, 36].

5. CONCLUSIONS

We have analyzed theoretically the optical response of a monolayer of regularly spaced quantum emitters with a doublet in the excited state (of the V-type) taking into account their total retarded dipole–dipole interaction, which is considered in the mean-field approximation. This interaction, due to its dependence on the current quantum state of an emitter, produces positive feedback, which, together with the immanent nonlinearity of emitters themselves, leads to multistability, periodic and aperiodic self-oscillations, and dynamic chaos in the optical response of the monolayer. Such a system can be implemented on the basis of supercrystals of semiconductor QDs with a degenerate valence band in a magnetic field [18] which gives rise to the Zeeman splitting of the conduction band of the quantum dot. Asymmetric semiconductor QDs, in which the anisotropic exchange interaction between an electron and a hole causes the doublet splitting of the one-exciton state (see, for example, [43]), can also serve as a model of a V-type quantum emitter.

For parameters of real supercrystals of semiconductor quantum dots, the frequencies of self-oscillations fall into the terahertz radiation range, i.e., the self-oscillation regime of the monolayer response is of interest for terahertz radiation sources. The sensitivity of the monolayer response to the initial conditions in the regime of dynamic chaos can be used for data encoding [44].

In a certain frequency range, the monolayer operates as a bistable mirror, i.e., its reflectance can be switched by a small variation of the external field amplitude from the state of almost total reflection to transmission. Analogous properties of 2D semiconductors (transition metals dichalcogenides) have recently been reported in publications [45, 46]. The (meta)monolayer of quantum emitters with the V-type scheme of operating optical transitions, considered in this study is another example of a nanometer-thick bistable mirror.

The above mentioned features of the nonlinear optical response of a monolayer of quantum emitters with a doublet in the excited state suggest promising applications in nanophotonics.

APPENDIX A

Solution of the Steady-State Problem

The steady-state solutions to the problem considered here ($\dot{\rho}_{\alpha\beta} = 0$, $\alpha, \beta = 1, 2, 3$) can be found by solving the following system off nonlinear algebraic equations:

$$(\gamma_{21} + 2\gamma_{32})Z_{31} - (2\gamma_{21} + \gamma_{32})Z_{21} - 3\mu(\Omega^*\rho_{21} + \Omega\rho_{21}^*) = \gamma_{21} - \gamma_{32}, \quad (22)$$

$$2(\gamma_{31} + \gamma_{32})Z_{31} - (\gamma_{31} + \gamma_{32})Z_{21} + 3(\Omega^*\rho_{31} + \Omega\rho_{31}^*) = -(\gamma_{31} + \gamma_{32}), \quad (23)$$

$$\Omega Z_{31} - \left[i\Delta_{31} + \frac{1}{2}(\gamma_{31} + \gamma_{32})\right]\rho_{31} + \mu\Omega\rho_{32} = 0, \quad (24)$$

$$\mu\Omega Z_{21} - \left(i\Delta_{21} + \frac{1}{2}\gamma_{21}\right)\rho_{21} + \Omega\rho_{32}^* = 0, \quad (25)$$

$$\mu\Omega^*\rho_{31} + \left[i\Delta_{32} + \frac{1}{2}(\gamma_{31} + \gamma_{21} + \gamma_{32})\right]\rho_{32} + \Omega\rho_{12}^* = 0, \quad (26)$$

$$\Omega = \Omega_0 + (\gamma_R - i\Delta_L)(\rho_{31} + \mu\rho_{21}), \quad (27)$$

where we used the substitution

$$\rho_{22} = \frac{1}{3}(1 - Z_{31} + 2Z_{21}), \quad \rho_{33} = \frac{1}{3}(1 + 2Z_{31} - Z_{21}).$$

Further, we define two vectors,

$$\mathbf{r} = (Z_{31}, Z_{21}, \rho_{31}, \rho_{21}, \rho_{32}, \rho_{31}^*, \rho_{21}^*, \rho_{32}^*),$$

$$\mathbf{r}_0 = (\gamma_{21} - \gamma_{32}, -(\gamma_{31} + \gamma_{32}), 0, 0, 0, 0, 0, 0).$$

The system of equations (22)–(26) can be written in the matrix form:

$$\mathcal{M}\mathbf{r}^T = \mathbf{r}_0^T, \quad (28)$$

where the superscript T indicates the transposition, and the explicit form of the matrix $\mathcal{M}_{ij}$, $i, j = 1, 2, ..., 8$ can easily be reconstructed from Eqs. (22)–(26). The formal solution to Eq. (28) reads

$$\mathbf{r}^T = \mathcal{M}^{-1}\mathbf{r}_0^T, \quad (29)$$

where the inverse matrix $\mathcal{M}^{-1}$ can be found in an explicit form. It should be emphasized that both $\mathcal{M}$ and $\mathcal{M}^{-1}$ and, accordingly, the solution to Eq. (29) depend parametrically on Ω. Having determined the vector $\mathbf{r}$, we can use it in (27) and obtain a closed equation for Ω. Knowing Ω, we can easily reconstruct all elements of the density matrix using Eq. (29) (see [16] for details). Thus, the steady-state problem is solved exactly.

APPENDIX B

Normal Modes of Dressed V-QE

As noted in Section 3.3, the optical transitions $1 \leftrightarrow 2$ and $1 \leftrightarrow 3$ in the dressed V-QE, first, acquire the frequency shifts and additional broadenings and, second, interact with each other due to the secondary field. We are interested in the normal modes of such a system in the linear case ($|\Omega_0| \ll 1$, $\rho_{11} \approx 1$). These modes can be found by solving the homogeneous problem ($\Omega_0 = 0$):

$$\dot{\rho}_{31} = [i\Delta_L - \Gamma_3]\rho_{31} - \mu(\gamma_R - i\Delta_L)\rho_{21}, \quad (30)$$

$$\dot{\rho}_{21} = [i(\Delta_{32} + \mu^2\Delta_L) - \Gamma_2]\rho_{21} - \mu(\gamma_R - i\Delta_L)\rho_{31}, \quad (31)$$

where we set $\Delta_{31} = 0$ and $\Delta_{21} = -\Delta_{32}$ (in zero external field) and introduced the notation

$$\Gamma_2 = \frac{1}{2}\gamma_{21} + \mu^2\gamma_R, \quad \Gamma_3 = \frac{1}{2}(\gamma_{31} + \gamma_{32}) + \gamma_R.$$

Further, let us seek the solution in the standard form $\rho_{\alpha\beta} = R_{\alpha\beta}\exp(\kappa t)$. Equating the determinant of the resultant system of algebraic equations to zero, we obtain the following equation for the eigenfrequencies of normal modes:

$$\kappa^2 - \{i[(1 + \mu^2)\Delta_L + \Delta_{32}] - \Gamma_2 - \Gamma_3\} + (i\Delta_L - \Gamma_3) \times [i(\Delta_{32} + \mu^2\Delta_L) - \Gamma_2] - \mu^2(\gamma_R - i\Delta_L)^2 = 0. \quad (32)$$

We do not write down here the cumbersome general expression for the roots $\kappa_\pm$ of Eq. (32) and restrict our analysis to the case of $\mu = 1$. Then

$$\kappa_\pm = \frac{1}{2}[i(2\Delta_L + \Delta_{32}) - \Gamma_2 - \Gamma_3] \pm \frac{1}{2}[(i\Delta_{32} + \Gamma_3 - \Gamma_2)^2 + 4(i\Delta_L - \gamma_R)^2]^{1/2}. \quad (33)$$

Further, we take into account the fact that under the conditions considered in this study, the value of Δ_L is much larger than the values of remaining quantities (Δ_{32}, Γ_2, Γ_3, and γ_R) so that one can use for $\kappa_\pm$ the expansion into the Taylor series in small parameters Δ_{32}/Δ_L, Γ_2/Δ_L, Γ_3/Δ_L, and γ_R/Δ_L. Under these assumptions, the expressions for the roots $\kappa_\pm$ take the form

$$\kappa_+ = i\left(2\Delta_L + \frac{1}{2}\Delta_{32}\right) - \frac{1}{2}(\Gamma_2 + \Gamma_3 + 2\gamma_R) = i\left(2\Delta_L + \frac{1}{2}\Delta_{32}\right) - \frac{1}{4}(\gamma_{21} + \gamma_{31} + \gamma_{32}) - 2\gamma_R, \quad (34)$$

$$\kappa_- = \frac{1}{2}i\Delta_{32} - \frac{1}{2}(\Gamma_2 + \Gamma_3 - 2\gamma_R) = \frac{1}{2}i\Delta_{32} - \frac{1}{4}(\gamma_{21} + \gamma_{31} + \gamma_{32}). \quad (35)$$

From here it follows that the bare frequencies $-\Delta_L$ and $-(\Delta_L + \Delta_{32})$ (see Eqs. (30) and (31)), detuned from each other by Δ_L, are radically renormalized due to the interaction: the frequencies of normal modes have values $-\Delta_{32}/2$ and $-(2\Delta_L + \Delta_{32}/2)$ and differ from each other by $2\Delta_L$. The relaxation constants of the normal modes are also modified considerably: the mode "+" now contains the double collective constant γ_R, while this constant is completely absent in the mode "–."

Using the algebraic equations for the amplitudes R_{31} and R_{21}, one can find the ratio R_{31}/R_{21} in the modes "+" and "–." Simple calculations show that

$$R_{31}^+/R_{21}^+ = 1 + O(\Delta_{32}/\Delta_L),$$

$$R_{31}^-/R_{21}^- = -1 + O(\Delta_{32}/\Delta_L),$$

i.e., the amplitudes R_{31} and R_{21} in the mode "+" are added in phase (symmetric, or bright mode), while in the mode "–," these amplitudes are added in antiphase (antisymmetric, or dark mode). This is precisely what determines the coupling (strong or weak) of these modes with the external field. The mode mixing depends linearly on the doublet splitting Δ_{32}. This is confirmed in the linear regime of reflection (see Fig. 6).

REFERENCES

1. N. I. Zheludev, Science (Washington, DC, U. S.) **328**, 582 (2010).
2. C. M. Soukoulis and M. Wegener, Science (Washington, DC, U. S.) **330**, 1633 (2010).
3. Y. Liu and X. Zhang, Chem. Soc. Rev. **40**, 2494 (2011).
4. W. H. Evers, B. Goris, S. Bals, M. Casavola, J. de Graaf, R. van Roij, M. Dijkstra, and D. Vanmaekelbergh, Nano Lett. **13**, 2317 (2013).
5. M. P. Boneschanscher, W. H. Evers, J. J. Geuchies, T. Altantzis, B. Goris, F. T. Rabouw, S. A. P. van Rossum, H. S. J. van der Zant, L. D. A. Siebbeles, G. van Tendeloo, I. Swart, J. Hilhorst, A. V. Petukhov, S. Bals, and D. Vanmaekelbergh, Science (Washington, DC, U. S.) **344**, 1377 (2014).
6. A. V. Baranov, E. V. Ushakova, V. V. Golubkov, A. P. Litvin, P. S. Parfenov, A. V. Fedorov, and K. Berwick, Langmuir **31**, 506 (2015).
7. W. Liu, X. Luo, Y. Bao, Y. P. Liu, G.-H. Ning, I. Abdelwahab, L. Li, C. T. Nai, Z. G. Hu, D. Zhao, B. Liu, S. Y. Quek, and K. P. Loh, Nat. Chem. **9**, 563 (2017).
8. A. S. Baimuratov, I. D. Rukhlenko, V. K. Turkov, A. V. Baranov, and A. V. Fedorov, Sci. Rep. **3**, 1727 (2013).
9. A. S. Baimuratov, I. D. Rukhlenko, and A. V. Fedorov, Opt. Lett. **38**, 2259 (2013).
10. A. S. Baimuratov, A. I. Shlykov, W. Zhu, M. Yu. Leonov, A. V. Baranov, A. V. Fedorov, and I. D. Rukhlenko, Opt. Lett. **42**, 2223 (2017).
11. I. A. Vovk, N. V. Tepliakov, A. S. Baimuratov, M. Yu. Leonov, A. V. Baranov, A. V. Fedorov, and I. D. Rukhlenko, Phys. Chem. Phys. **20**, 25023 (2018).
12. J. F. Nossa and A. S. Camacho, Microelectron. J. **38**, 1251 (2008).
13. A. S. Baimuratov, Y. K. Gun'ko, A. V. Baranov, A. V. Fedorov, and I. D. Rukhlenko, Sci. Rep. **6**, 23321 (2016).
14. R. Malikov, I. Ryzhov, and V. Malyshev, Eur. Phys. J. Web Conf. **161**, 02014 (2017).
15. V. A. Malyshev, P. Á. Zapatero, A. V. Malyshev, R. F. Malikov, and I. V. Ryzhov, J. Phys.: Conf. Ser. **1220**, 012006 (2019).
16. I. V. Ryzhov, R. F. Malikov, A. V. Malyshev, and V. A. Malyshev, Phys. Rev. A **100**, 033820 (2019).
17. I. Ryzhov, R. Malikov, A. Malyshev, and V. Malyshev, Eur. Phys. J. Web Conf. **220**, 02012 (2019).
18. Al. L. Efros, M. Rosen, M. Kuno, M. Nirmal, D. J. Norris, and M. Bawendi, Phys. Rev. B **54**, 4843 (1996).
19. D. Bayramdurdiyev, R. Malikov, I. Ryzhov, and V. Malyshev, Eur. Phys. J. Web Conf. **220**, 03004 (2019).
20. R. A. Vlasov, A. M. Demeza, and M. G. Gladush, J. Appl. Spectrosc. **80**, 698 (2013).
21. R. A. Vlasov, A. M. Lemeza, and M. G. Gladush, Laser Phys. Lett. **10**, 045401 (2013).
22. G. Lindblad, Comm. Math. Phys. **48**, 119 (1976).
23. K. Blum, *Density Matrix: Theory and Applications* (Springer, Berlin, 2012).
24. R. H. Dicke, Phys. Rev. **93**, 99 (1954).
25. R. F. Malikov, E. D. Trifonov, and A. I. Zaitsev, Sov. Phys. JETP **49**, 33 (1979).
26. M. G. Benedict, A. M. Ermolaev, V. A. Malyshev, I. V. Sokolov, and E. D. Trifonov, *Super-Radiance: Multiatomic Coherent Emission* (IOP, Bristol, 1996).
27. J.-P. Eckmann and D. Ruelle, Rev. Mod. Phys. **57**, 617 (1985).
28. A. Katok and B. Hasselblatt, *Introduction to the Modern Theory of Dynamical Systems* (Cambridge Univ. Press, Cambridge, 1997).
29. A. A. Andronov, A. A. Vitt, and S. E. Khaikin, *Theory of Oscillators* (Pergamon, New York, 1966).
30. J. Guckenheimer and P. Holmes, *Nonlinear Oscillations, Dynamical Systems and Bifurcations of Vector Fields* (Springer, Berlin, 1986).
31. V. S. Afrajmovich, Yu. S. Il'yashenko, and L. P. Shil'nikov, *Dynamical Systems V: Bifurcation Theory and Catastrophe Theory*, Ed. by V. I. Arnol'd (Springer, Berlin, 1994).
32. Y. Ben-Aryeh, C. M. Bowden, and J. C. Englund, Phys. Rev. A **34**, 3917 (1086).
33. S. M. Zakharov and E. A. Manykin, Poverkhnost', No. 2, 137 (1988).
34. A. M. Basharov, Sov. Phys. JETP **67**, 1131 (1988).
35. M. G. Benedikt, A. I. Zaitsev, V. A. Malyshev, and E. D. Trifonov, Opt. Spectrosc. **68**, 473 (1990).
36. M. G. Benedict, A. I. Zaitsev, V. A. Malyshev, and E. D. Trifonov, Phys. Rev. A **43**, 3845 (1991).
37. A. N. Oraevsky, D. J. Jones, and D. K. Bandy, Opt. Commun. **111**, 163 (1994).
38. V. A. Malyshev and E. Conejero Jarque, Opt. Experess **6**, 227 (2000).
39. H. Glaeske, V. A. Malyshev, and K.-H. Feller, J. Chem. Phys. **113**, 1170 (2000).
40. J. A. Klugkist, V. A. Malyshev, and J. Knoester, J. Chem. Phys. **127**, 164705 (2007).
41. R. F. Malikov and V. A. Malyshev, Opt. Spectrosc. **122**, 955 (2017).
42. R. F. Malikov and V. A. Malyshev, Eur. Phys. J. Web Conf. **161**, 03005 (2017).
43. S. Stufler, P. Machnikowski, P. Ester, M. Bichler, V. M. Axt, T. Kuhn, and A. Zrenner, Phys. Rev. B **73**, 125304 (2006).
44. T. Gao and Z. Chen, Phys. Lett. A **372**, 394 (2008).
45. P. Back, S. Zeytinoglu, A. Ijaz, M. Kroner, and A. Imamoğlu, Phys. Rev. Lett. **120**, 037401 (2018).
46. G. Scuri, Y. Zhou, A. A. High, D. S. Wild, C. Shu, K. de Greve, L. A. Jauregui, T. Taniguchi, K. Watanabe, P. Kim, M. D. Lukin, and H. Park, Phys. Rev. Lett. **120**, 037402 (2018).

Translated by N. Wadhwa